A nuclear envelope protein linking nuclear pore basket assembly, SUMO protease regulation, and mRNA surveillance

Alaron Lewis,[1] Rachael Felberbaum,[2] and Mark Hochstrasser[3]

Departments of [1]Cell Biology; [2]Molecular, Cell, and Developmental Biology; and [3]Molecular Biophysics and Biochemistry, Yale University, New Haven, CT 06520

The nuclear pore complex (NPC) is both the major conduit for nucleocytoplasmic trafficking and a platform for organizing macromolecules at the nuclear envelope. We report that yeast Esc1, a non-NPC nuclear envelope protein, is required both for proper assembly of the nuclear basket, a structure extending into the nucleus from the NPC, and for normal NPC localization of the Ulp1 SUMO protease. In *esc1Δ* cells, Ulp1 and nuclear basket components Nup60 and Mlp1 no longer distribute broadly around the nuclear periphery, but co-localize in a small number of dense-staining perinuclear foci. Loss of Esc1 (or Nup60) alters SUMO conjugate accumulation and enhances *ulp1* mutant defects. Similar to previous findings with Mlp1, both Esc1 and Ulp1 help retain unspliced pre-mRNAs in the nucleus. Therefore, these proteins are essential for proper nuclear basket function, which includes mRNA surveillance and regulation of SUMO protein dynamics. The results raise the possibility that NPC-localized protein desumoylation may be a key regulatory event preventing inappropriate pre-mRNA export.

Introduction

Covalent attachment to polypeptide modifiers is a common means of regulating protein function (Schwartz and Hochstrasser, 2003). Ubiquitin is the prototypical member of this group of small protein modifiers, called ubiquitin-like proteins (Ubls). Small ubiquitin-related modifier (SUMO) is the most extensively studied Ubl other than ubiquitin itself. SUMO attachment to a protein can change its distribution, activity, and/or binding partners, and sumoylated proteins function in processes as diverse as cytokinesis, transcription, DNA repair, and chromosome segregation (Melchior et al., 2003; Schwartz and Hochstrasser, 2003; Johnson, 2004). Whether or not a given substrate becomes sumoylated is influenced by a variety of factors, including subcellular localization of the substrate and enzymes responsible for attaching and removing SUMO from the substrate, phase of the cell cycle, redox state, or DNA damage (Pfander et al., 2005; Takahashi et al., 2005; Bossis and Melchior, 2006; Kerscher et al., 2006).

The levels of sumoylated substrates reflect a balance between rates of SUMO conjugation and deconjugation. Conjugation of SUMO to proteins requires a series of enzymes related to the E1, E2, and E3 enzymes that activate and transfer ubiquitin to its substrates. SUMO protein modification is highly dynamic. Removal of SUMO from proteins as well as SUMO precursor processing requires specialized proteases called SUMO proteases or desumoylating enzymes. The known desumoylating enzymes are conserved from yeast to humans, forming part of a clan of specialized cysteine proteases (Li and Hochstrasser, 1999). In yeast, SUMO (encoded by the *SMT3* gene) is cleaved from its substrates by one of two desumoylating enzymes, Ulp1 or Ulp2 (Smt4) (Li and Hochstrasser, 1999, 2000). Ulp1 is also the primary SUMO precursor processing enzyme. Many of the components of the SUMO pathway, including Ulp1, are essential for viability.

Protein–SUMO ligation can be regulated by alteration of the substrate, such as phosphorylation, or by alteration of the SUMO-modifying enzymes, such as the control of E1 and E2 activity through redox signaling (Bossis and Melchior, 2006). Regulation of SUMO protease activity is less well understood. Subcellular localization appears to be a key determinant.

A. Lewis and R. Felberbaum contributed equally to this paper.

Correspondence to Mark Hochstrasser: mark.hochstrasser@yale.edu

Alaron Lewis' present address is Department of Biochemistry, University of Washington, Seattle, WA 98195.

Abbreviations used in this paper: Mlp, myosin-like protein; NPC, nuclear pore complex; SUMO, small ubiquitin-related modifier; ts, temperature sensitive; UD, Ulp catalytic domain; WT, wild type.

The online version of this article contains supplemental material.

The Journal of Cell Biology, Vol. 178, No. 5, August 27, 2007 813–827
http://www.jcb.org/cgi/doi/10.1083/jcb.200702154

Saccharomyces cerevisiae Ulp2 and its known substrates are found within the nucleus (Bachant et al., 2002; Stead et al., 2003). In contrast, Ulp1 is localized primarily to the nuclear pore complex (NPC) (Li and Hochstrasser, 2000; Schwienhorst et al., 2000), and this localization is crucial for proper control of protein desumoylation (Li and Hochstrasser, 2003; Panse et al., 2003; Zhao et al., 2004). Sequestration of Ulp1 at NPCs appears to prevent it from desumoylating Ulp2 substrates in vivo inasmuch as it can readily cleave SUMO from many of these proteins in vitro (Li and Hochstrasser, 2000, 2003).

The NPC is a large protein complex that spans the nuclear envelope and allows the regulated passage of macromolecules between the nucleus and cytoplasm (Tran and Wente, 2006). It also helps organize chromatin and various protein complexes to facilitate gene expression, DNA repair, and other nuclear functions (Therizols et al., 2006; Tran and Wente, 2006). Ulp1 is among a small group of proteins that concentrates at a subset of NPCs: unlike most NPC proteins, it is largely excluded from the nuclear envelope region abutting the nucleolus (Zhao et al., 2004). Ulp1 associates with the NPC through its noncatalytic N-terminal domain, which includes a coiled coil and distinct binding sites for two karyopherin nuclear transport factors. The upstream karyopherin-binding site in Ulp1 interacts with Kap121 (Pse1), a karyopherin involved in mRNA export from the nucleus (Panse et al., 2003). The second site binds Kap60-Kap95, the karyopherin α-β heterodimer responsible for import of proteins bearing a classical nuclear localization signal (NLS). Removal of a single karyopherin-binding element affects Ulp1 localization only moderately, whereas removal of both elements leads to an enzymatically active C-terminal fragment that localizes throughout the nucleus and can be toxic (Mossessova and Lima, 2000; Li and Hochstrasser, 2003; Panse et al., 2003).

Other proteins that contribute to Ulp1 localization are the myosin-like proteins Mlp1 and Mlp2 and the nucleoporin Nup60 (Zhao et al., 2004). In the absence of Mlp1/2 or Nup60, levels of Ulp1 are significantly decreased and the remaining protein, while still partially localized to the NPC, is no longer excluded from the nucleolar region, indicating a change in Ulp1–NPC interaction (Zhao et al., 2004). Nup60 and Nup1 are the only nucleoporins (Nups) that are found exclusively on the nuclear side of the NPC, and they contribute to a filamentous structure called the nuclear basket, which extends into the nucleoplasm (Rout et al., 2000; Denning et al., 2001). The nuclear basket provides binding sites for many proteins entering and exiting the NPC. Notably, Nup60 binds the mobile nucleoporin Nup2 that is responsible for recycling Kap60 (karyopherin α) from the nucleus back to the cytoplasm (Denning et al., 2001; Dilworth et al., 2001; Matsuura et al., 2003). Mlp1 and Mlp2 are also associated with the nuclear basket. Mlp1 has recently been linked to a novel RNA quality-control pathway that prevents leakage of unspliced pre-mRNA from the nucleus (Galy et al., 2004; Palancade et al., 2005). Normally, incompletely spliced mRNA precursors are retained in the nucleus until splicing is completed; failure to do so can lead to translation of aberrant proteins (Vinciguerra and Stutz, 2004). Cells lacking Nup60 are also defective in this pathway.

In this study, we demonstrate that the nuclear envelope protein Esc1 is required for the proper assembly and localization of the nuclear basket. Esc1 is a large coiled-coil protein that associates with the inner nuclear membrane but is not part of the NPC (Andrulis et al., 2002; Taddei et al., 2004). Esc1 binds and localizes the silencing factor Sir4. Genetic loci subject to chromatin-mediated silencing, such as telomeres, localize to the nuclear periphery and bind a complex of Sir (silent information regulatory) proteins (Taddei et al., 2004). Concentration of Sir4 at the nuclear periphery can facilitate silencing. Sir4 is anchored at the nuclear membrane by binding either Esc1 or another protein complex, Yku70-Yku80; these proteins play redundant roles in tethering Sir4 and silent chromatin to nuclear envelope sites, and both contribute to telomeric silencing (Andrulis et al., 2002; Taddei et al., 2004).

We find that Esc1, by controlling nuclear basket assembly, also modulates Ulp1 localization at the nuclear envelope. In *esc1Δ* cells, Nup60 and Ulp1 colocalize in aberrant, bright-staining foci at the nuclear periphery. The *esc1Δ* and *nup60Δ* mutations have similar effects on SUMO conjugate accumulation and interact similarly with *ulp1* and *ulp2* mutations. Deletion of *ESC1* suppresses *ulp2Δ*, but this does not require Sir4 or the peripheral anchoring of silent chromatin. Collectively, our data show that Esc1 is essential for normal nuclear basket assembly and helps functionally segregate the Ulp1 and Ulp2 proteases.

Loss of Esc1 also causes a defect in the retention of unspliced pre-mRNA in the nucleus similar to that seen in *mlp1Δ* cells. The function of Esc1 and Mlp1 in preventing such aberrant RNA export is genetically linked, and in *esc1Δ* cells, Mlp1 is mislocalized to perinuclear aggregates. Notably, Ulp1 is also required for normal nuclear pre-mRNA retention, by a mechanism genetically linked to Esc1 and Mlp1. These results suggest that Ulp1 activity at the NPC is integral to the surveillance of mRNA export.

Results

Loss of Esc1 partially suppresses *ulp2Δ* mutant defects

Deletion of the Ulp2 SUMO protease causes a variety of defects, including slow growth, sensitivity to high temperature, and permanent cell cycle arrest in response to DNA or spindle damage (Li and Hochstrasser, 2000). Previous studies had shown that *ulp2Δ* defects could be suppressed by mutations in other SUMO pathway components, including mutations in the Ulp1 SUMO protease that decrease its activity or prevent it from concentrating at the NPC (Li and Hochstrasser, 2000, 2003). Ulp1 mislocalization may allow it to gain access to substrates that are normally desumoylated only by Ulp2.

To identify additional proteins that are components or regulators of the SUMO pathway, including factors required for the proper localization of Ulp1, we devised a genomic screen based on suppression of *ulp2Δ*. The screen was performed using the synthetic genetic array (SGA) method in which the mutant of interest, *ulp2Δ*, was crossed to the ordered array of ∼4,800 nonessential gene deletion mutants assembled in the *S. cerevisiae*

Genome Project (Tong et al., 2001). After sporulation, haploid double mutants were selected and screened for suppression of *ulp2Δ* defects. Double mutants were tested under three conditions: high temperature (37°C), DNA damage by hydroxyurea (0.1 M HU), and microtubule destabilization by benomyl (10 μg/ml). The *ulp2Δ* single mutant shows little or no growth under each of these conditions. After a series of secondary screens, a total of 49 potential *ulp2Δ* suppressors were identified. These suppressors affected proteins that participate in a variety of cellular processes, including protein translation, lipid synthesis, mitochondrial energy production and chromatin regulation. We decided to focus on the eight mutants affecting proteins linked to chromatin function. By tetrad analysis, four of the eight had suppressor mutations unlinked to the original deletion allele. Of the remaining four mutants, only *esc1Δ* showed consistent suppression of *ulp2Δ* defects in all double mutant segregants.

To verify that *ulp2Δ* suppression was due specifically to loss of Esc1, a new *esc1Δ* mutant was constructed in the W303 genetic background and was mated to a congenic *ulp2Δ* strain. The resulting diploids were sporulated and dissected, and tetrads were evaluated for growth. As expected, the *ulp2Δ* single mutant grew poorly or not at all under the tested conditions, and *esc1Δ* cells grew similarly to wild type (WT) (Fig. 1 A). The *ulp2Δ esc1Δ* cells showed enhanced growth at 37°C and on benomyl when compared with *ulp2Δ*. However, the irregular colony size and slow growth at 24°C and HU sensitivity associated with *ulp2Δ* were not suppressed.

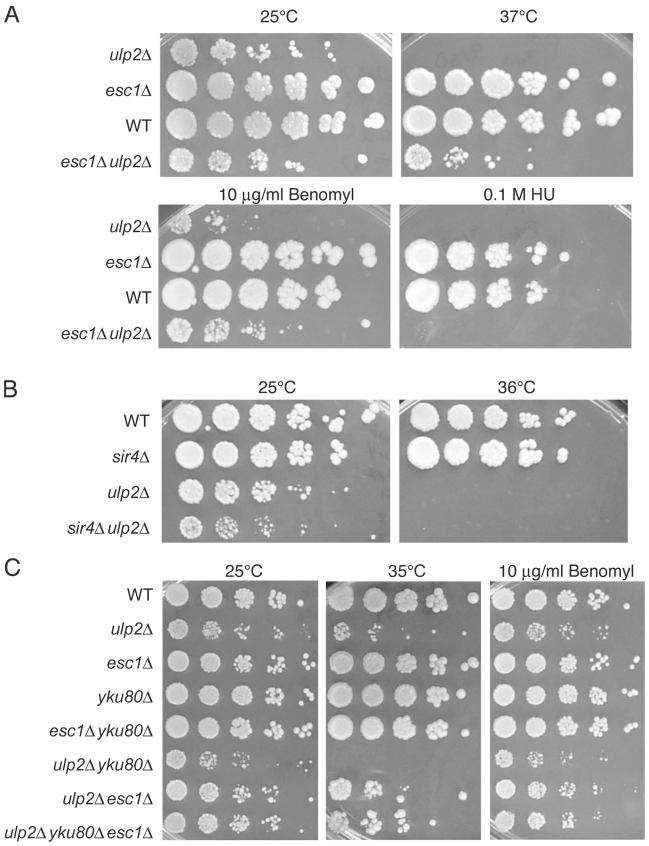

Figure 1. **Temperature and benomyl sensitivity of *ulp2Δ* cells are partially suppressed by *esc1Δ*.** (A) Five-fold serial dilutions of yeast cultures were spotted onto YPD or the indicated media and grown for 3–5 d. Drug plates were grown at 24°C. (B) Deletion of the silencing factor Sir4 does not suppress *ulp2Δ*. (C) The heterodimer Yku80/Yku70, which functions redundantly with Esc1 in localizing Sir4 to the nuclear periphery, does not interact genetically with *ulp2Δ*.

Loss of gene silencing does not suppress *ulp2Δ*

Esc1 is one of two proteins that bind and concentrate the silencing factor Sir4 at the nuclear periphery, thereby enhancing telomeric silencing (Andrulis et al., 2002; Taddei et al., 2004). Were *ulp2Δ* suppression caused by a defect in silencing, then *sir4Δ*, which causes a complete loss of silencing, should suppress *ulp2Δ* at least as well as *esc1Δ*. This was not the case: a *sir4Δ ulp2Δ* double mutant showed no suppression of the temperature-sensitive (ts) phenotype as compared with the *ulp2Δ* single mutant and even slightly enhanced the growth defect at 25°C (Fig. 1 B). Thus, loss of silencing does not suppress *ulp2Δ*.

It was still possible that delocalization of Sir4 was the source of the suppression. To test this, we inactivated the other factor involved in Sir4 peripheral localization, the Yku70-Yku80 heterodimer. In *yku80Δ*, as in *esc1Δ*, Sir4 is partially mislocalized; while in the *esc1Δ yku80Δ* double deletion, Sir4 is diffusely distributed throughout the nucleus (Taddei et al., 2004). The *yku80Δ* mutant cannot grow at 37°C, so suppression of *ulp2Δ* was tested at 35°C, where *yku80Δ* cells grow similarly to WT (Fig. 1 C). Mutant *yku80Δ ulp2Δ* cells did not show suppression of either the ts growth or benomyl sensitivity of *ulp2Δ* (Fig. 1 C). In fact, the double mutant grew worse than *ulp2Δ* at 35°C, presumably due to the loss of other functions of Yku80 (Taddei et al., 2004). Full delocalization of Sir4 in *ulp2Δ yku80Δ esc1Δ* cells did not enhance suppression beyond what was seen with *ulp2Δ esc1Δ* (Fig. 1 C). We conclude that the role of Esc1 in the SUMO pathway is independent of its function in silencing or Sir4 localization.

Esc1 is required for proper Ulp1 distribution

Our earlier work had shown that mutations in Ulp1 which prevented it from localizing correctly to the NPC could suppress some defects associated with *ulp2Δ* (Li and Hochstrasser, 2003). Given the position of Esc1 at the nuclear envelope, we examined the possibility that *ESC1* deletion might affect anchoring of Ulp1 to the NPC. Cells lacking *ULP1* were complemented with a low-copy plasmid expressing *ULP1-GFP* under the control of the *ULP1* promoter. In WT cells, Ulp1-GFP localized in a broadly distributed punctate pattern around the nuclear periphery but was excluded from the presumptive juxta-nucleolar region, as expected (Fig. 2 A). Unexpectedly, in *esc1Δ* cells, most Ulp1-GFP accumulated in a small number of bright foci that still appeared to be at the nuclear periphery (this was also observed with chromosomally integrated *ULP1-GFP*; not depicted). Subsequent experiments confirmed that the foci were on the nuclear envelope, and in many cases, some residual staining could be seen around the nucleus outside of the bright foci (see Fig. 5 A).

Foci were prominent in many, but not all of the optical sections of *esc1Δ* nuclei. Therefore, foci frequency was quantified. Nuclei were scored as having foci if they included at least

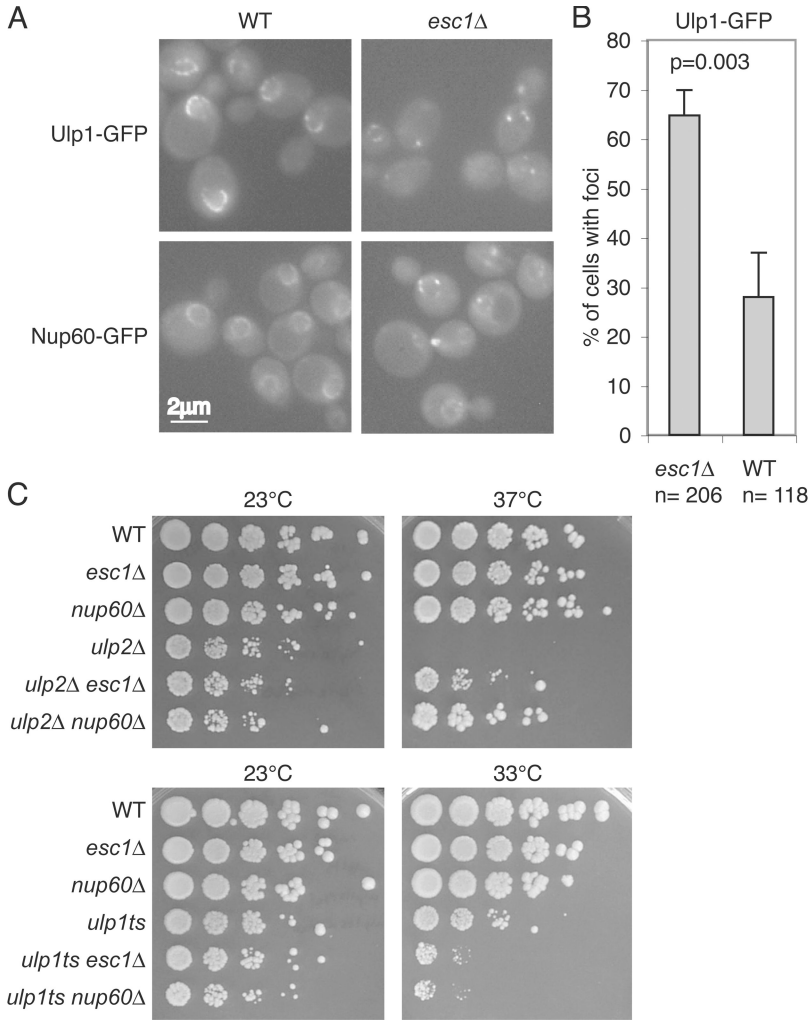

Figure 2. **Loss of Esc1 causes mislocalization of Ulp1 and the Nup60 nucleoporin.** (A) Cells expressing either Ulp1-GFP or Nup60-GFP were examined by fluorescence microscopy. Both Ulp1 and Nup60 accumulate in foci on the nuclear periphery in *esc1Δ* cells. (B) Ulp1-GFP foci counts in WT and *esc1Δ* cells. Cells with one or more bright spots were scored as containing foci. Pictures were counted from three separate experiments and >100 cells were counted for each genotype. Error bars represent standard deviations between datasets. A paired *t* test was used to evaluate the significance of the difference in foci frequency between the two genotypes. (C) Similar to *esc1Δ*, deletion of Nup60, a nuclear basket protein, suppresses the temperature-sensitive growth of *ulp2Δ* (top panels). Both *esc1Δ* and *nup60Δ* showed a mild synthetic interaction with the *ulp1-3-33* ts allele. Dilution series were prepared as in Fig. 1.

one dense Ulp1-GFP spot on the nuclear periphery. Using this measure, 64% of Ulp1-GFP–expressing *esc1Δ* cells had foci compared with 28% in WT (Fig. 2 B).

Esc1 function and the NPC nuclear basket

Esc1 does not colocalize with the NPC (Andrulis et al., 2002; Taddei et al., 2004), raising the question of how Esc1 can influence the distribution of Ulp1, which is mostly NPC bound. The yeast nucleoporin Nup60 localizes strictly to the nuclear side of the NPC and is a major constituent of the nuclear basket; Nup60 is known to be required for proper localization of Ulp1 (Zhao et al., 2004). These observations suggested that Esc1 might influence Ulp1 (and Ulp2) function by altering the nuclear basket of the NPC.

We first asked whether proper nuclear basket assembly or localization depends on Esc1. In WT cells, Nup60-GFP (expressed from the endogenous *NUP60* locus) localized broadly around the nuclear periphery, as expected (Fig. 2 A). Strikingly, in *esc1Δ* cells, Nup60-GFP concentrated in bright foci on the nuclear periphery, very similar to the foci seen with Ulp1 (Fig. 2 A; also see Fig. 4). Because Ulp1 was mislocalized in both the *esc1Δ* and *nup60Δ* mutants, we asked if *nup60Δ* and *esc1Δ* had comparable genetic interactions with mutations in the Ulp1 and Ulp2 SUMO proteases. As was true for *esc1Δ*, *nup60Δ* partially suppressed the ts lethality of *ulp2Δ*; in fact, *nup60Δ ulp2Δ* grew even better at high temperature than did *esc1Δ ulp2Δ* (Fig. 2 C). The irregular colony growth of *ulp2Δ*, measured at 24°C, was not altered by either *esc1Δ* or *nup60Δ*. In contrast, when combined with a ts-allele of *ULP1*, both *esc1Δ* and *nup60Δ* caused an enhanced growth defect at the *ulp1ts* semi-permissive temperature of 33°C (Fig. 2 C). We do not know why *nup60Δ* was not identified in our original *ulp2Δ* suppressor screen.

Mutation of either the Ulp1 or Ulp2 SUMO protease causes an increase in the sumoylation levels of specific substrates; prominent changes are detectable by anti-SUMO immunoblot analysis of whole cell lysates (Li and Hochstrasser, 2000; Bylebyl et al., 2003). If loss of Nup60 or Esc1 were affecting either SUMO protease activity, changes in the cellular SUMO protein pattern might also be seen. However, unlike *ulp* cells, neither *nup60Δ* nor *esc1Δ* displayed a strong increase in the general level of sumoylated proteins, suggesting that both Ulps retained substantial activity in these nuclear envelope mutants (Fig. 3, lanes 1–3, 10–12).

On the other hand, weak but reproducible changes in the intensity of several bands were detected (marked by asterisks;

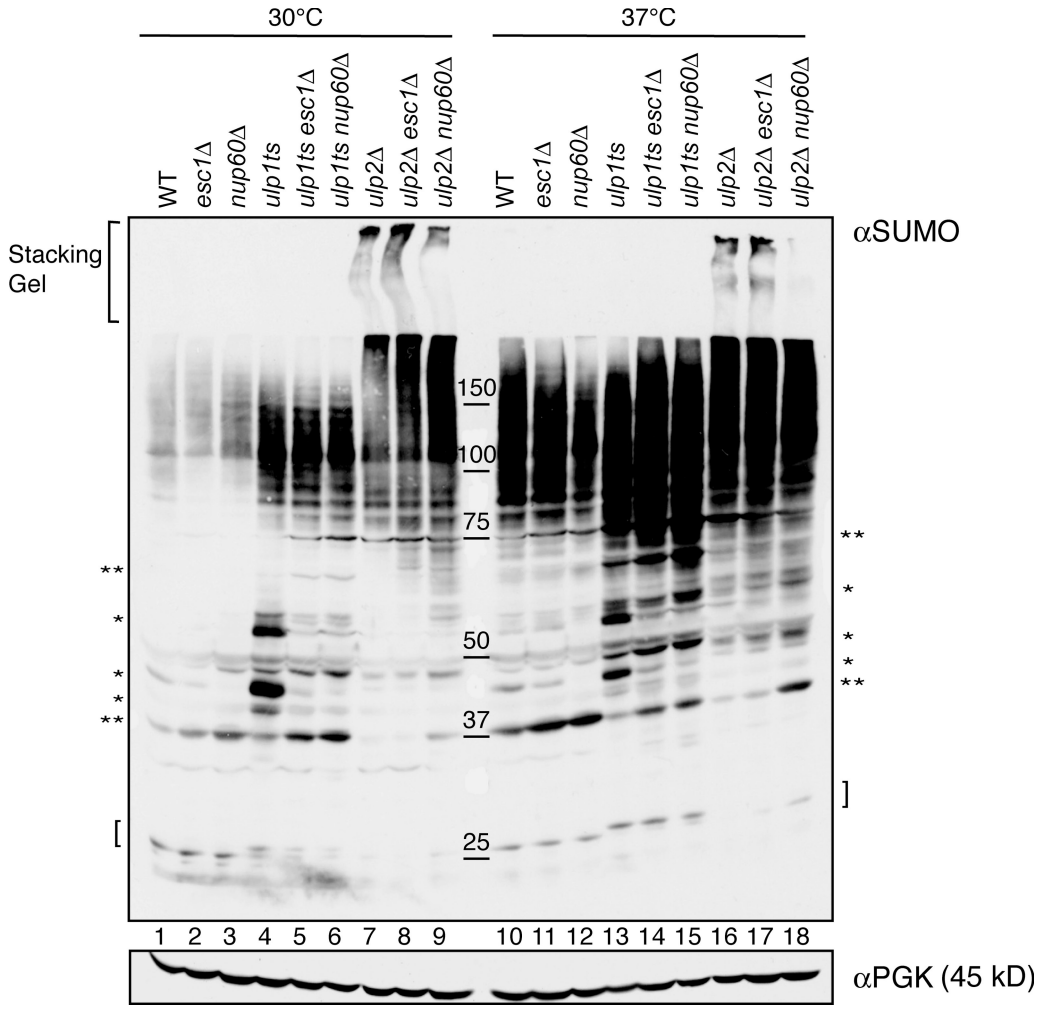

Figure 3. **Both *esc1Δ* and *nup60Δ* cause subtle changes in SUMO protein conjugate profiles, particularly in the *ulp1ts* mutant.** Cells were shifted from 30°C to the indicated temperature for 4 h and then lysed in TCA. Proteins were separated on a 6–15% gradient polyacrylamide gel and assayed by anti-SUMO immunoblotting. A single asterisk marks sumoylated species that decrease in level in *esc1Δ* and *nup60Δ* mutants. Two asterisks indicate species that increase in these mutants. The bracket indicates the position of free SUMO and the unprocessed SUMO precursor in the *ulp1ts* strain. PGK, phosphoglycerate kinase (loading control).

some only clearly seen with longer film exposures). Interestingly, the small changes observed in the *nup60Δ* and *esc1Δ* SUMO conjugate profiles were generally amplified when these gene deletions were combined with *ulp1ts*, but not when combined with *ulp2Δ* (Fig. 3). This implied that the majority of detectable sumoylated proteins affected by loss of either Nup60 or Esc1 were Ulp1 substrates, consistent with a primary role for these proteins in Ulp1 localization. The alteration of only a subset of sumoylated proteins and the observation that specific sumoylated species either increased or decreased in abundance suggested that the *nup60Δ* and *esc1Δ* mutations changed the ability of Ulp1 to act on particular substrates. No obvious changes to the profile of high-molecular mass SUMO conjugates in *ulp2Δ* cells were observed when either *nup60Δ* or *esc1Δ* was introduced, although it is possible that changes to individual substrates might have been obscured by other intensely stained species. Levels of polysumoylated species detected in the stacking gel from *ulp2Δ*-derived extracts (lanes 7–9, 16–18) varied between experiments but were always present. Conceivably, the phenotypic suppression of *ulp2Δ* by loss of either Nup60 or Esc1 might be a consequence of changes in the levels of Ulp1-specific SUMO protein substrates.

In summary, the data in Figs. 2 and 3 indicate first, that mutations in Nup60 and Esc1 have similar interactions with Ulp1 and Ulp2 mutations, consistent with a close link between Esc1 and nuclear basket function, and second, that Ulp1 and Nup60 both accumulate in similar structures when Esc1 is deleted. These results suggest that mislocalization of Ulp1 likely underlies the genetic interactions of *nup60Δ* and *esc1Δ* with mutations in the Ulp2 protease.

Ulp1 and NPC protein recruitment to *esc1Δ* foci

Loss of Esc1 caused both Nup60 and Ulp1 to concentrate in bright foci at the nuclear periphery. If Esc1 was affecting Ulp1 through changes in Nup60 assembly or localization, then Nup60 and Ulp1 should colocalize to the same foci in the *esc1Δ* mutant.

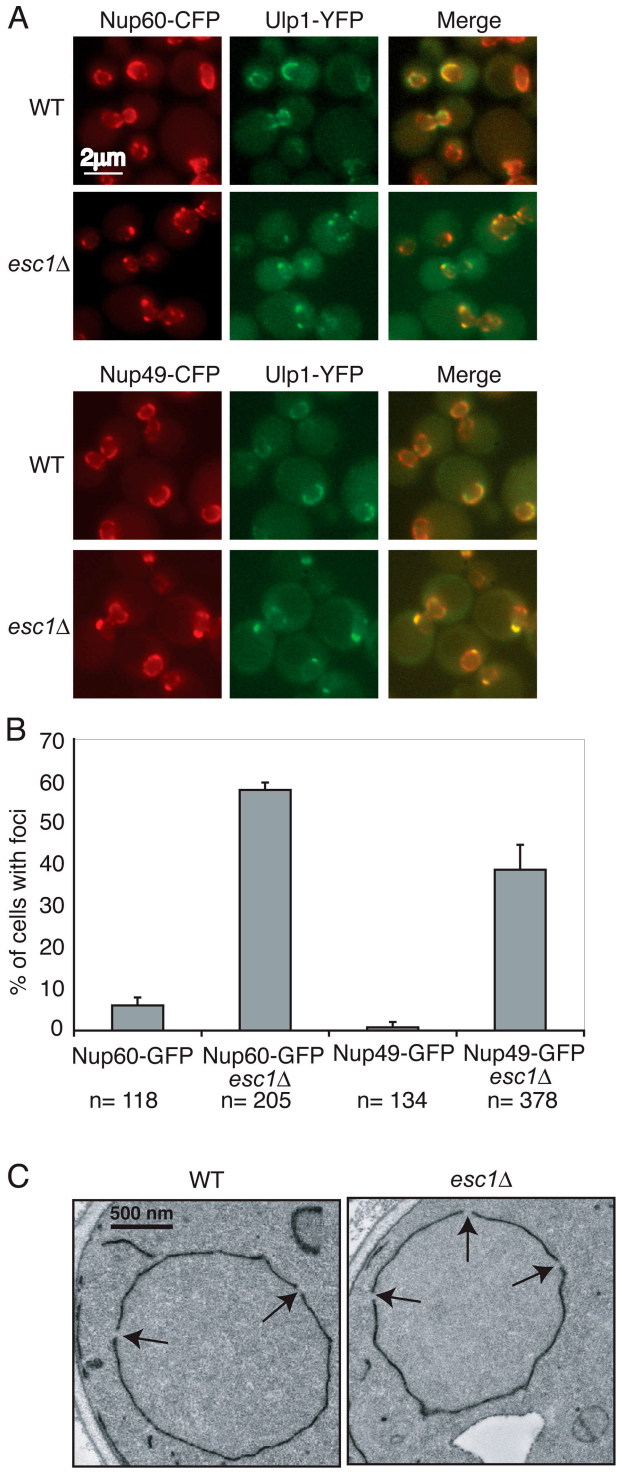

Figure 4. **Other nucleoporins also accumulate in *esc1Δ* foci.** (A) Co-localization of proteins analyzed in cells with integrated *NUP-CFP* constructs and expressing Ulp1-YFP from a plasmid in otherwise WT cells. (B) Cells containing either Nup60-GFP or Nup49-GFP fusions were scored as in Fig. 2 B for the presence of foci. The decreased number of foci and increased variability in Nup49-GFP foci compared with Nup60-GFP foci correlated with greater persistence of normally localized Nup49-GFP even in foci-containing cells. (C) Electron microscopy revealed no obvious nuclear morphology defects or NPC clustering in *esc1Δ* cells. Cells were fixed with glutaraldehyde followed by $KMnO_4$. Nuclear pores are marked with arrows.

This was investigated in cells coexpressing Nup60-CFP and Ulp1-YFP fusion proteins (Fig. 4 A). In WT cells, Ulp1 appeared to colocalize with Nup60, as predicted if both are part of, or associate with, the NPC. In *esc1Δ* cells, all the bright Ulp1-YFP foci also stained strongly with Nup60-CFP. Controls using each of these tags individually showed no fluorescence in the opposite channel (not depicted).

Mislocalization of Nup60 to foci in *esc1Δ* cells could result from either specific aggregation of nuclear basket components and associated proteins or a general mislocalization of the entire NPC. To distinguish between these two possibilities, we examined the localization of Nup49, a core nucleoporin found within the central rings of the NPC (Strambio-de-Castillia and Rout, 2002). In an *esc1Δ* strain with the endogenous *NUP49* locus tagged with either *GFP* or *CFP*, localization of Nup49 was perturbed but to a lesser extent than either Nup60 or Ulp1. Specifically, Nup49 showed an increase in the level of bright foci on the nuclear periphery, but it also continued to show a broad punctate localization to the nuclear periphery (Fig. 4 A and Fig. 5). GFP fusions of Nup159 or Nsp1, two other nucleoporins, gave similar results, with Nup159, a component of the cytoplasmic NPC fibrils, showing only modest redistribution (Fig. S1 A, available at http://www.jcb.org/cgi/content/full/jcb.200702154/DC1). The degree of mislocalization of Nup60 and Nup49 was quantified, and we found that 58% of *esc1Δ* cells had Nup60-GFP foci and 39% had Nup49-GFP foci (Fig. 4 B).

The accumulation of other nucleoporins in the *esc1Δ*-induced foci, albeit not to the same extent as Nup60 or Ulp1, suggested that loss of Esc1 might cause a general clustering of NPCs. To investigate this idea, we examined nuclear pore distribution in electron micrographs of permanganate-fixed cells from WT and *esc1Δ* cells; the conditions were chosen to enhance visualization of membranes. Fig. 4 C shows a representative cell of each cell type. No gross nuclear membrane abnormalities were visible in *esc1Δ*. A limited analysis of pore distribution was performed in which distances between pores were measured for at least eight cells of each strain (180 pores). By comparing the distances between pores in the two strains, the distribution of pores was not significantly altered in the *esc1Δ* cells ($p = 0.29$). Therefore, full NPCs appear not to undergo gross redistribution, even though some of their components aggregate into peripheral foci. Future studies using different types of EM sample preparation might identify the foci detected by fluorescence microscopy and allow their ultrastructural characterization.

Nup60-dependent protein accumulation in *esc1Δ* foci

Given the more complete redistribution of Nup60 to *esc1Δ* foci when compared with other nucleoporins, it was possible that aggregated nuclear basket components (Nup60) misrouted other nucleoporins to the foci by protein–protein interactions that normally occur in NPCs. This hypothesis predicts that eliminating Nup60 from *esc1Δ* cells would prevent accumulation of core nucleoporins in foci. Indeed, in an *esc1Δ nup60Δ* double mutant, we found that Nup49-GFP was localized normally to

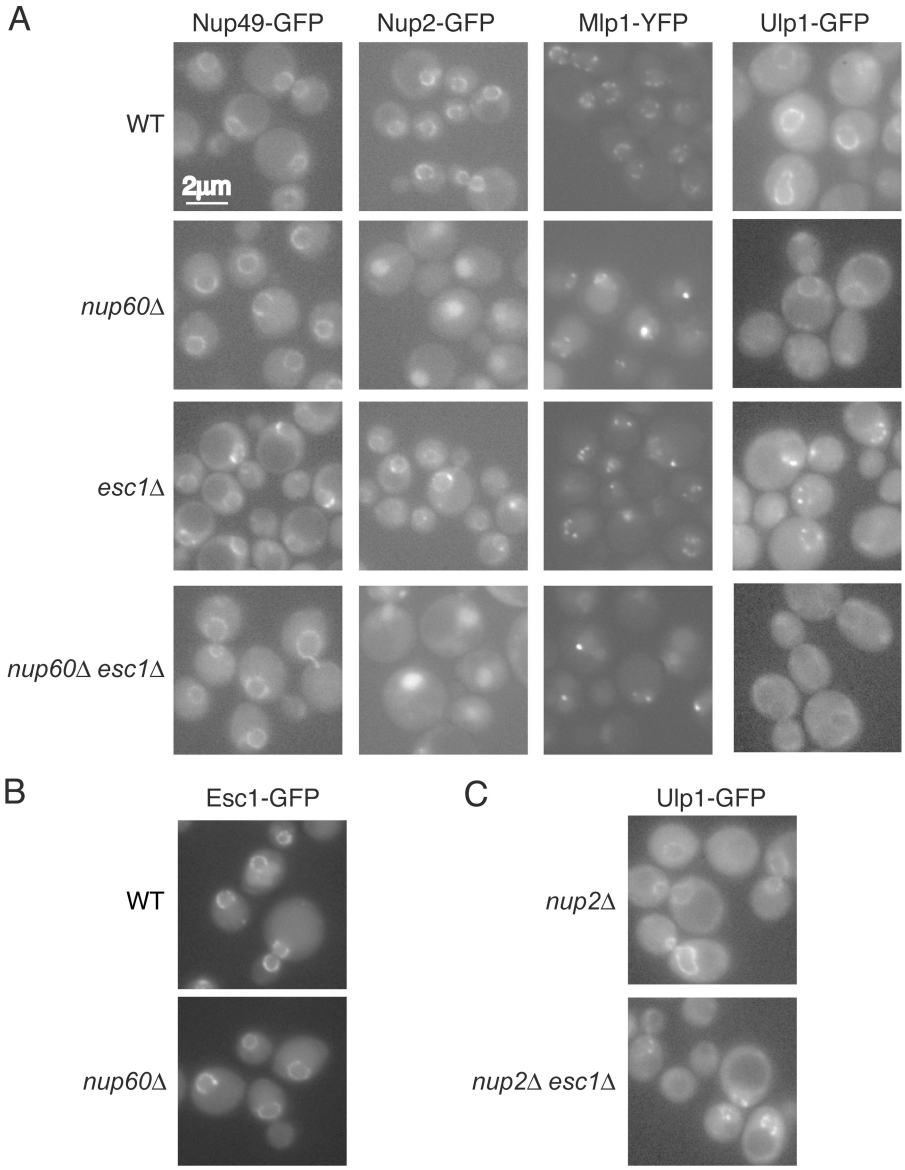

Figure 5. **Nucleoporin and NPC-associated protein accumulation in foci of *esc1Δ* and *esc1Δ nup60Δ* cells.** (A) Nup49-GFP, Nup2-GFP, Mlp1-YFP, and Ulp1-GFP accumulate in *esc1Δ* foci but this requires Nup60. Deletion of Nup60 causes depletion of Ulp1, as expected. (B) Esc1-GFP localization is not altered by *nup60Δ*. (C) Deletion of *NUP2* does not change Ulp1 localization in WT or *esc1Δ* cells. *ULP1-GFP* was expressed from the *ULP1* promoter on a plasmid in WT cells.

the nuclear periphery and no longer accumulated in foci (Fig. 5 A). The *nup60Δ* single mutant did not change Nup49-GFP localization, nor did it alter Esc1-GFP distribution (Fig. 5 B). These results suggest that Esc1 is not directly required for proper nuclear membrane distribution of NPCs, but instead prevents formation of Nup60-containing aggregates that can recruit other NPC components.

To examine the ability of Nup60 in *esc1Δ* foci to bind one of its direct NPC-binding partners, we looked at the localization of Nup2. Nup2 is a mobile nucleoporin that is required for the recycling of Kap60 from the nucleus to the cytoplasm (Dilworth et al., 2001; Matsuura et al., 2003). On the nuclear side of the NPC, Nup2 binds to Nup60. In *nup60Δ* mutants, Nup2 was diffusely distributed in the nucleus, as expected (Fig. 5 A). In *esc1Δ* cells, Nup2 localized to foci, similar to the other tested nucleoporins, while in the *esc1Δ nup60Δ* double mutant, it was dispersed within the nucleus, as in the *nup60Δ* single mutant. This suggests that Nup60 is still able to contact its normal interacting partners in the *esc1Δ* foci, consistent with the requirement for Nup60 in misrouting nucleoporins such as Nup49 to these foci. Finally, localization of Ulp1 to *esc1Δ* foci also depended on Nup60 because the low level of remaining Ulp1-GFP seen in *esc1Δ nup60Δ* cells was diffusely distributed with residual nuclear rim staining (Fig. 5 A).

Nup60 is known to interact with the Kap60-Kap95 heterodimer via Nup2 (Denning et al., 2001; Dilworth et al., 2001). As noted earlier, the Kap60-Kap95 complex can bind to Ulp1, so Nup60-dependent Ulp1 localization to *esc1Δ* foci might be mediated by Nup2. However, we found that deletion of *NUP2* did not reduce localization of Ulp1 to the dense perinuclear foci (Fig. 5 C), indicating that Nup2 is not essential for Ulp1 localization to these sites.

The related Mlp1 and Mlp2 proteins also associate with the nuclear basket (Feuerbach et al., 2002). When we examined Mlp1-YFP localization in *esc1Δ* cells, the protein concentrated in foci that were qualitatively similar to Nup60 and Ulp1 foci in this mutant (Fig. 5 A). In cells lacking Nup60, Mlp1-YFP is known to aggregate into 1–2 large perinuclear foci (Feuerbach et al., 2002;

Palancade et al., 2005). These foci are fewer in number and larger than those seen in *esc1Δ* cells (Fig. 5 A). In the *esc1Δ nup60Δ* double mutant, the foci are indistinguishable from the foci in the *nup60Δ* single mutant, indicating that *nup60Δ* is epistatic to *esc1Δ* for Mlp1 localization as well as for Ulp1 localization. Notably, Nup60 localization to the NPC did not depend on Mlp1/2 (Fig. S1 B).

In summary, these localization data argue that Esc1 limits nuclear basket (Nup60) aggregation. In the absence of Esc1, Nup60 accumulates in foci and recruits other components of the NPC and basket-associated proteins such as Nup2, Mlp1, and Ulp1.

The coiled-coil domain of Ulp1 is required for localization to *esc1Δ* foci

Ulp1 has two distinct karyopherin-binding sites and a coiled-coil region in its N-terminal noncatalytic domain (Li and Hochstrasser, 2003; Panse et al., 2003). We used Ulp1 derivatives lacking one or more of these elements to determine their importance for Ulp1 localization to foci in *esc1Δ* cells (Fig. 6 A). The proteins were fused to a 9-myc epitope tag and expressed from the *ULP1* promoter on low-copy plasmids; the full-length tagged protein has WT function under these conditions (Li and Hochstrasser, 2003). Levels of Ulp1 were similar in *ESC1* and *esc1Δ* cells based on immunoblotting (Fig. S3, available at http://www.jcb.org/cgi/content/full/jcb.200702154/DC1). All constructs were expressed in *ulp1Δ* cells except *ulp1Δ418-621* and *ulp1Δ347-621*, which were expressed in WT cells because these derivatives lack the essential catalytic domain (UD) and thus are unable to complement *ulp1Δ* lethality.

As seen previously, the catalytic domain of Ulp1 was dispensable for NPC localization: the ulp1Δ418-621 protein lacking the UD localized to the nuclear envelope and was recruited to foci in *esc1Δ* cells (Fig. 6 B). However, ulp1Δ347-621, which differs from ulp1Δ418-621 by the absence of the coiled-coil domain, while still mostly concentrated at the nuclear periphery, did not form foci in *esc1Δ* cells. Persistent envelope localization of ulp1Δ347-621 in *ESC1* cells (Fig. 6 B) and of full-length Ulp1 in *nup60Δ* cells (Fig. 5 A) is consistent with a second, Nup60-independent binding mechanism of Ulp1 to the NPC (Panse et al., 2003; Zhao et al., 2004). These data and the lack of Ulp1 foci in *nup60Δ esc1Δ* cells suggest that localization to *esc1Δ* foci provides a stringent test for Nup60-dependent NPC localization and that the Ulp1 coiled coil is crucial for this.

Ulp1 constructs containing only the karyopherin Kap121 or the Kap60-Kap95 binding site are partially delocalized from the nuclear periphery (Panse et al., 2003). Despite their inability to localize fully to NPCs in *ESC1* cells, Ulp1 derivatives missing one or the other of the karyopherin-binding sites (ulp1Δ2-144 and ulp1Δ150-346) still localized at least partially to foci in *esc1Δ* cells (Fig. 6 B). All constructs lacking the coiled coil (ulp1Δ150-403, ulp1Δ346-403, and ulp1Δ347-621) failed to incorporate into *esc1Δ* foci. Notably, the NPC localization defect of ulp1Δ150-403 in *ESC1* cells was more severe than that of ulp1Δ150-346, suggesting a contribution of the coiled coil to NPC localization in *ESC1* cells as well. Conversely, ulp1Δ2-346, which has only the coiled-coil and the catalytic domain, was diffusely localized, mostly in the nucleus, in both *ESC1* and *esc1Δ* cells, indicating that the coiled-coil domain, while necessary, is not sufficient for localization to foci or for full localization to NPCs.

Esc1 helps prevent leakage of unspliced pre-mRNA from the nucleus

The myosin-like protein Mlp1 functions in an RNA quality-control pathway that retains unspliced pre-mRNAs in the nucleus (Galy et al., 2004). We asked whether *esc1Δ*, which causes mislocalization of Mlp1 to perinuclear foci (Fig. 5 A), also compromises this specific RNA retention mechanism. Using a plasmid (pJCR1) encoding an inefficiently spliced intron-containing *lacZ* reporter designed to allow translation of β-galactosidase (β-Gal) only if the unspliced pre-mRNA is transported to the cytoplasm (Galy et al., 2004) (Fig. 7 A), we found that the relative level of β-Gal activity in *esc1Δ* cells reached a level similar to β-Gal activity in an *mlp1Δ* mutant (Fig. 7 B). Interfering with splicing by mutation of the branchpoint sequence (mutBP) in the intron leads to increased leakage of unspliced pre-mRNA from the nucleus in WT cells, and leakage of this mutant pre-mRNA is greatly enhanced in *mlp1Δ* cells (Galy et al., 2004). We observed a similar enhancement of leakage of the splicing-defective message in the *esc1Δ* mutant (Fig. 7 B). Using a *lacZ* reporter (pJCR51) in which β-Gal is produced only from the correctly spliced mRNA (Galy et al., 2004), no defect in pre-mRNA splicing was observed in either *mlp1Δ* or *esc1Δ* (Fig. S2, available at http://www.jcb.org/cgi/content/full/jcb.200702154/DC1). When *mlp1Δ* and *esc1Δ* were combined, the level of aberrant pre-mRNA export in the double mutant did not exceed what was observed in the single mutants, arguing that Esc1 acts in the same RNA surveillance pathway as Mlp1 (Fig. 7 C).

Finally, we asked if mislocalization or reduced activity of Ulp1 might be linked to aberrant pre-mRNA leakage as well. Mislocalization of the active Ulp1 catalytic domain (ulp1-C204) to the nuclear interior (Li and Hochstrasser, 2003) did not cause increased leakage (not depicted). However, *ulp1ts* cells, which have substantially reduced Ulp1 activity even at permissive temperature (Li and Hochstrasser, 1999), suffer levels of pre-mRNA leakage comparable to *esc1Δ* cells (Fig. 7 D). When the *ulp1ts* mutation was combined with *esc1Δ*, the extent of pre-mRNA leakage was not significantly higher than in the single mutants (Fig. 7 D). These data are consistent with the possibility that aggregation of Ulp1 in *esc1Δ* foci impairs Ulp1 function and that a reduction of SUMO protease activity at the NPC contributes to the RNA surveillance defect of the *esc1Δ* and *mlp1Δ* mutants. We note that fusion of the Ulp1 catalytic domain to three different nucleoporins (Nup60, Nsp1, or Nup42; Panse et al., 2003) failed to suppress pre-mRNA leakage in either *mlp1Δ* or *ulp1ts* cells (unpublished data). There are various potential explanations for these negative results; for example, elements of Ulp1 in addition to its catalytic domain might be necessary for this pathway.

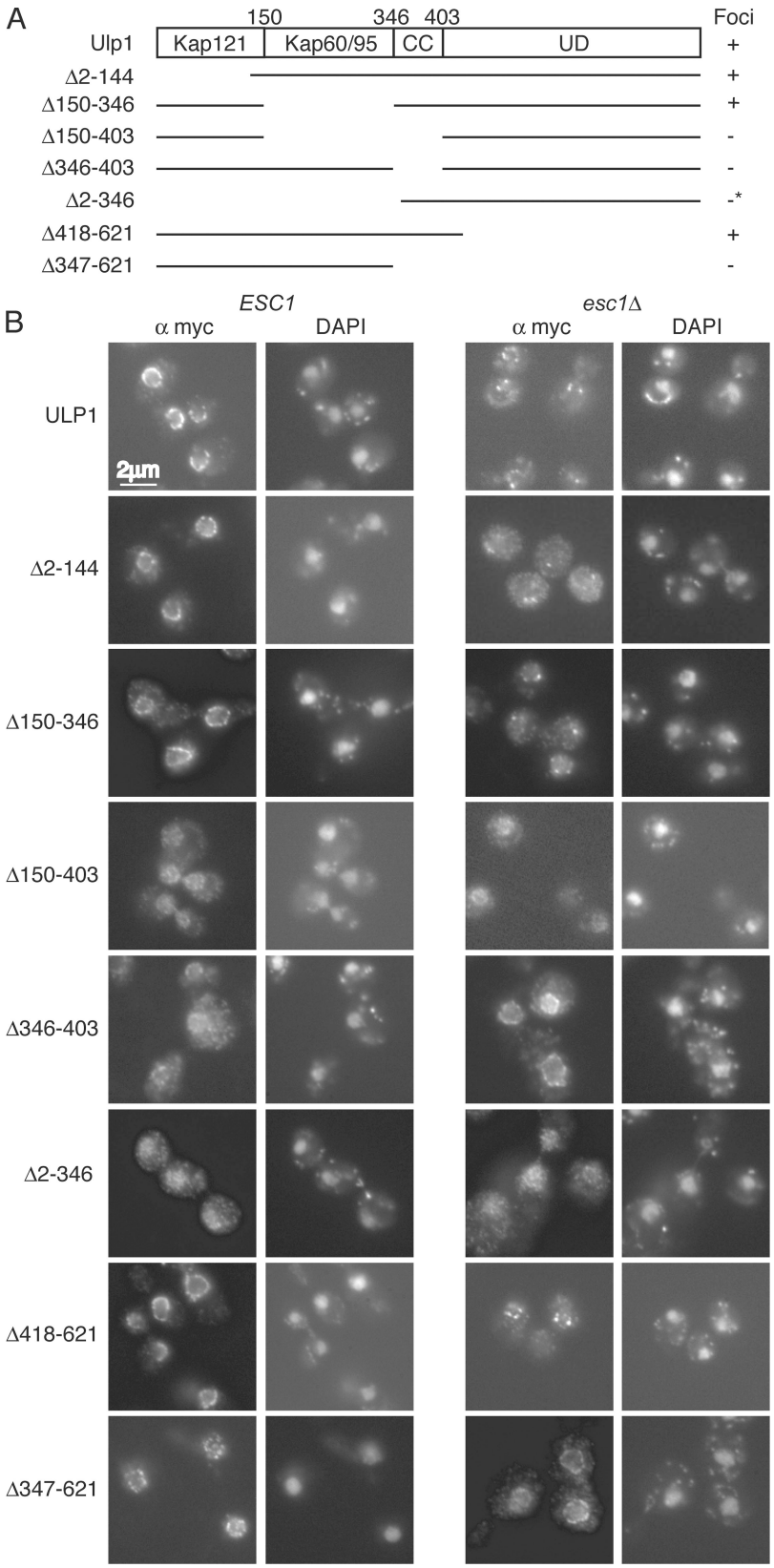

Figure 6. **The coiled-coil domain of Ulp1 is required for Ulp1 localization to *esc1Δ* foci.** (A) Schematic of Ulp1 deletion constructs used and summary of immunofluorescence localization results. The two domains labeled Kap121 and Kap60/95 denote binding sites for these karyopherins. CC represents a coiled-coil domain, and UD marks the catalytic or Ulp domain. All constructs bear a C-terminal 9-myc tag, and were localized by indirect immunofluorescence. Constructs lacking the UD domain were expressed in *ULP1* cells. All other constructs were expressed in *ulp1Δ* cells. *, the Δ2-346 construct was localized diffusely within the nucleus in both *ESC1* and *esc1Δ* cells. (B) Immunofluorescence images of Ulp1-myc derivatives expressed in *ESC1* and *esc1Δ* cells. Anti-myc staining shows Ulp1 localization, while DAPI stains DNA.

Discussion

We have found that the non-NPC protein Esc1 is required for the proper assembly of NPC nuclear baskets at the yeast nuclear envelope. Nuclear basket assembly, in turn, is necessary for proper localization and regulation of the Ulp1 SUMO protease. Mislocalization of Ulp1 partially overcomes defects associated with loss of the nuclear SUMO protease Ulp2. Our results

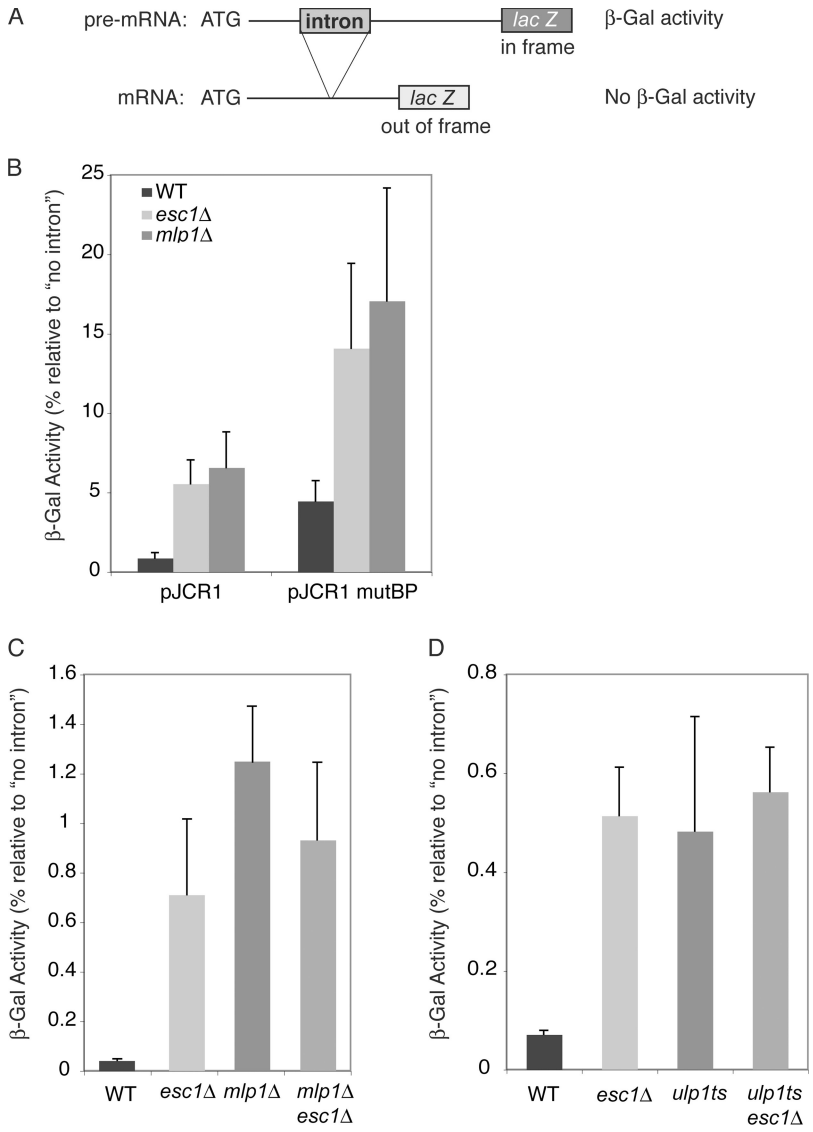

Figure 7. **Esc1 and Ulp1 help retain unspliced pre-mRNAs in the nucleus.** (A) Schematic of *lacZ* reporter (pJCR1) used for measuring pre-mRNA leakage. (B) β-galactosidase (β-Gal) activity from pre-mRNA leakage reporters (pJCR1 and pJCR1mutBP) relative to β-Gal activity of a control *lacZ* reporter lacking introns (pLGSD5). Error bars show SDs (three independent transformants tested for each genotype). (C) Comparison of pre-mRNA leakage in the *mlp1Δ esc1Δ* double mutant and single mutants. Assays were done as in B. Activity ratios varied some from those in panel B primarily as a result of differences in the "no intron" baseline values. (D) Ulp1 is required for normal pre-mRNA retention. Assays were done as in B.

reveal an unexpected network of interactions at the nuclear envelope that modulate both the distribution of NPC components and the dynamics of SUMO protein conjugation. Comparison to findings with the human SUMO protease SENP2/hULP2 and nuclear envelope factors suggests conservation of these nuclear envelope interactions. Finally, both Esc1 and Ulp1 are required for preventing aberrant export of unspliced pre-mRNAs from the nucleus, suggesting an important role for Esc1-dependent nuclear basket organization and Ulp1-dependent protein desumoylation in this RNA surveillance pathway.

Esc1, nuclear basket assembly, and parallels to the vertebrate nucleus

Ultrastructural data from vertebrate cells indicate that the nuclear basket comprises a series of long fibrils emanating from the nuclear ring of the NPC and extending into the nucleus to a distal ring (Fahrenkrog and Aebi, 2003). Two proteins in *S. cerevisiae*, Nup1 and Nup60, are known to localize exclusively to the nuclear side of the NPC and are thought to be constituents of the nuclear basket. Mlp1 and Mlp2 are more distally located from the inner nuclear membrane and are either part of or are tightly associated with the nuclear basket (Rout et al., 2000). Mlp1 and Mlp2 require Nup60 for their tethering to the NPC. The likely mammalian homologue of Mlp1/2 is Tpr, and Tpr is a major architectural component of the mammalian nuclear basket (Krull et al., 2004). Tpr is anchored to the nuclear side of the NPC by the nuclear basket protein Nup153, a protein with many functional similarities to yeast Nup60 (Hase and Cordes, 2003).

S. cerevisiae does not have a morphologically detectable nuclear lamina, nor has an obvious yeast lamin orthologue been identified. However, the localization of Esc1 at the yeast inner nuclear membrane regions between NPCs, the presence of multiple heptad repeats in Esc1, and the apparent lipid modification of Esc1 suggest that Esc1 might be a functional counterpart to the lamins or lamin-associated proteins of metazoans (Andrulis et al., 2002; Taddei et al., 2004). Our data strengthen this possibility. Esc1 is required for proper assembly and distribution of Nup60 into nuclear baskets on the nuclear face of NPCs. Based on experiments with *Xenopus* egg extracts, Nup153 (the potential orthologue of yeast Nup60) requires nuclear

lamina formation for its proper assembly and maintenance in the NPC basket (Smythe et al., 2000). In human cells, the likely orthologue of Ulp1, SENP2 (hULP2), associates directly with Nup153 (Hang and Dasso, 2002; Zhang et al., 2002). Our data with *esc1Δ* cells demonstrate that Ulp1 aggregates along with Nup60 into perinuclear foci but that such localization of Ulp1 is lost if Nup60 is also deleted (Fig. 5 A). Whether Ulp1 binds directly to Nup60 or to Mlp1/2 or both sets of proteins is not yet known. Our results suggest, first, that nuclear basket association is a conserved feature of yeast Ulp1 and human SENP2 (hULP2) and, second, that the vertebrate lamina, like the perinuclear yeast Esc1 protein, is likely to have a substantial impact on SUMO protease subcellular distribution and function.

Previous studies of Ulp1 identified two binding sites in the N terminus of the protein that bind to the karyopherins Kap121 and Kap60-Kap95, respectively (Panse et al., 2003). The accumulation of Ulp1 into Nup60-dependent foci in an *esc1Δ* mutant gave us the opportunity to explore the role of karyopherin binding in the Nup60-dependent localization of Ulp1. We found that while the presence of at least one karyopherin-binding site was required, the adjacent coiled-coil domain was also essential for the accumulation of Ulp1 in foci. The karyopherins that bind Ulp1 associate only transiently with the NPC and are also localized throughout the nucleus and cytoplasm. How an interaction with such mobile proteins could lead to the concentration of Ulp1 at the NPC was unclear. Our data suggest that karyopherin binding, while important for Ulp1 localization, is not sufficient. Association with karyopherins might help bring Ulp1 to the nuclear basket, but binding to Nup60, Mlp1/2, or other components of the basket is likely to be necessary to keep it there.

SUMO protease localization and sumoylation dynamics

The non-NPC Esc1 protein is required for proper localization of the Ulp1 SUMO protease to the NPC, but we identified *esc1Δ* from a screen for suppressors of the *ulp2Δ* mutant. Suppression of *ulp2Δ* defects can be accomplished either by decreasing the rate of SUMO conjugation or by increasing the ability of the other yeast desumoylating enzyme, Ulp1, to access Ulp2 substrates (Li and Hochstrasser, 2000, 2003; Bylebyl et al., 2003). Ulp1 normally appears to be limited from desumoylating Ulp2 substrates by its association with the NPC (Li and Hochstrasser, 2003). In *esc1Δ* cells, Ulp1 concentrated at dense foci on the nuclear periphery, suggesting that the suppression of *ulp2Δ* by this mutant might be due to a change in Ulp1 localization or activity. Supporting this interpretation, we found very similar SUMO conjugate profiles in *esc1Δ* and *nup60Δ* mutants, and both mutations had similar genetic interactions with *ulp1* and *ulp2* mutations. The *nup60Δ* mutation is known to cause mislocalization and reduced levels of Ulp1 (Fig. 5 A; Zhao et al., 2004). Consistent with the idea of reduced Ulp1 activity in *esc1Δ* cells, both *esc1Δ* and *ulp1ts* cells behaved similarly in pre-mRNA leakage assays, and combining the two mutant alleles did not further enhance the extent of leakage (Fig. 7 D).

Despite the partial suppression of *ulp2Δ* mutant defects, however, the SUMO conjugate patterns of *ulp2Δ nup60Δ* and *ulp2Δ esc1Δ* double mutants were not grossly different from that of the *ulp2Δ* single mutant. Suppression might result from effects on a specific subset of Ulp2 substrates, potentially ones of low abundance. Loss of Nup60 might suppress *ulp2Δ* by increasing amounts of Ulp1 in the nuclear interior or by reducing Ulp1 levels (Zhao et al., 2004). In the *esc1Δ* mutant, aggregation of Ulp1 into peripheral foci could decrease Ulp1 activity sufficiently to mimic a mutation that partially inactivates its SUMO protease activity, which is known to suppress *ulp2Δ* defects (Li and Hochstrasser, 2000), or a small amount of Ulp1 could mislocalize to the nucleoplasm and cleave certain Ulp2 SUMO-conjugated substrates. The fact that suppression of *ulp2Δ* benomyl- and temperature-sensitivity is modest, and other *ulp2Δ* defects are not suppressed, is consistent with the limited changes observed in bulk SUMO conjugates. An alternative but not mutually exclusive explanation of *ulp2Δ* suppression is that certain sumoylated proteins are uniquely cleaved by Ulp1 or Ulp2, but these different substrates may function in the same cell regulatory pathway(s). Hence, a change in the sumoylation level of a Ulp1-specific substrate might affect the phenotype of *ulp2Δ* cells indirectly by altering such a pathway.

Esc1 and Ulp1 help prevent egress of unspliced mRNAs from the nucleus

Ribonucleoprotein (RNP) export from the nucleus is thought to involve docking of the RNP to the distal ring of the nuclear basket, movement into the basket, and then transport across the core NPC into the cytoplasm (Soop et al., 2005). Despite the involvement of the nuclear basket in this process, its disruption in yeast by mutation of Nup60 causes at most only minor general nuclear transport defects (Denning et al., 2001). On the other hand, perturbation of nuclear basket structure by deletion of Nup60 or Mlp1 allows aberrant export of intron-containing mRNPs without an overall increase in mRNP export (Galy et al., 2004). These results suggest a checkpoint function for Mlp1 and the nuclear basket in regulating mRNP export (Green et al., 2003). Given the functional connection that we found between Esc1 and the nuclear basket, we tested whether Esc1 might also contribute to this mRNP surveillance mechanism. Indeed, our data indicate that Esc1 also helps retain unspliced pre-mRNA in the nucleus and that Esc1 and Mlp1 function in the same pathway.

How unspliced pre-mRNAs are distinguished from mature mRNAs at the NPC remains speculative (Vinciguerra and Stutz, 2004). Two other proteins known to participate in the pathway are Pml1 and Pml39. Pml1 is part of a trimeric complex called RES (retention and splicing); unlike the other two subunits in RES, Pml1 has only a minimal role in pre-mRNA splicing but has an impact on pre-mRNA leakage comparable to that of Mlp1 (Dziembowski et al., 2004). Pml39 is anchored to Mlp1/2 and may aid in binding mRNPs. In contrast to Pml39, Esc1 does not require Nup60 for its proper localization at the nuclear envelope (Fig. 5 B). This implies that Esc1 functions in the assembly and organization of the nuclear basket, rather than the other way around, and that the disruption of basket assembly leads to the *esc1Δ* pre-mRNA leakage phenotype. The clustering or aggregation of Nup60 and Mlp1 into dense

perinuclear foci that are partially dissociated from the core NPCs may remove a barrier at the NPC that would normally retain unspliced mRNAs. This might involve mislocalization of the Ulp1 SUMO protease, the first enzyme that has been linked to this pre-mRNA surveillance pathway. Although the relevant targets of Ulp1 in such a checkpoint mechanism remain to be determined, a number of RNA export-linked proteins have been identified by proteomic analysis of sumoylated proteins (Hannich et al., 2005).

Materials and methods

Synthetic genetic array (SGA) screen

The screen was performed as described previously (www.utoronto.ca/boonelab/protocols.htm). The gene deletion library, which was assembled by the *S. cerevisiae* Genome Project and contained ~4,800 nonessential gene deletions, was purchased from Open Biosystems. The *ULP2* deletion strain was purchased as a heterozygote from the American Type Culture Collection.

Yeast strains and plasmids

Yeast strains and plasmids used in this study are listed in Tables I and II. Standard media and techniques were used for the growth and construction of yeast strains (Guthrie and Fink, 1991). For fluorescence microscopy, strains were grown in SD minimal media containing 0.04 g/L adenine.

Plasmids with three new *ULP1* deletion derivatives were made for this study: *ulp1-Δ150-403*, *ulp1-Δ346-403*, and *ulp1-Δ150-346*. Each was generated by homologous recombination in yeast using cotransformation of a linearized copy of YCplac22-ULP1-9myc along with a PCR product that contained *ULP1* sequences that flanked the deleted *ULP1* sequence and spanned the restriction site used to linearize YCplac22-Ulp1-9myc. For *ulp1-Δ150-403* and *ulp1-Δ105-346*, the plasmid was linearized with MscI, and for *ulp1-Δ346-403*, the linearized plasmid was gel-purified from a partial SacI digest.

Anti-SUMO immunoblotting

Cells were grown overnight in YPD, diluted to an OD_{600} of 0.2 and grown for an additional 4 h at either 30°C or 37°C. A volume of culture corresponding to 2.0 OD_{600} equivalents of cells was centrifuged for 30 s at 13,000 rpm. Cells were washed once in 20% TCA (Sigma-Aldrich) and resuspended in 400 µl 20% TCA and an equal volume of glass beads. Cells were vortexed on a Turbo Mix bead beater (Scientific Industries Inc.) for 4 min at 4°C. Supernatant was removed from the beads and centrifuged at 14,000 rpm for 10 min at 4°C. The pellet was washed with 2% TCA and resuspended in SDS gel-loading buffer. One OD_{600} equivalent of sample was loaded per lane on a 6–15% gradient polyacrylamide gel. After electrophoresis, proteins were transferred to a PVDF membrane and blocked with 10% nonfat dry milk in TBST (150 mM NaCl, 10 mM Tris-HCl pH 8.0, and 0.1% Tween 20) for 30 min, then incubated with anti-Smt3 (SUMO) antibody (1:5,000 in 1% nonfat dry milk in TBST; Li and Hochstrasser, 1999) or anti-PGK 22C5 antibody (1:7,000 in 1% nonfat dry milk in TBST; Molecular Probes) for 2 h at room temperature. Membranes were washed three times with TBST for 10 min each, and incubated with donkey anti–rabbit antibody (1:6,000 in 1% nonfat dry milk in TBST; Amersham Biosciences) or goat anti–mouse IgG_1 (γ1) antibody (1:10,000 in 1% nonfat dry milk in TBST; Roche) for 1 h. Membranes were washed three times in TBST for 10 min each and ECL detection reagents were added as directed by the manufacturer (Amersham Biosciences) and exposed to film.

Fluorescence microscopy

Cells were grown in SD media to an OD_{600} of 0.3–0.8, placed on a slide and viewed on a microscope (Axioskop; Carl Zeiss MicroImaging, Inc.) with a plan-Apochromat 100× NA1.4 objective lens at room temperature using Zeiss immersion oil IMMERSOL 518F. Pictures were taken on a Zeiss Axiocam camera using a Uniblitz shutter driver (model VMM-D1; Vincent Associates) and the program Open Lab 3.1.5 (Improvision).

For indirect immunofluorescent staining with anti-myc antibodies, cells were grown overnight in SD medium lacking tryptophan. They were then diluted and grown to an OD_{600} of 0.6–1.0. Ten ml of culture were collected by centrifugation, resuspended in 1 ml 3.7% formaldehyde, and incubated while shaking at 30°C for 90 min. Cells were pelleted at 2,000 rpm for 2 min, washed twice in Buffer B (0.1 M KPO_4), and resuspended in Buffer C (1.2 M sorbitol, 0.1 M KPO_4). Cells were often kept at 4°C overnight at this point. Cells were incubated while rotating at 30°C for 40 min in 1 ml Buffer C with 2.5 µl β-mercaptoethanol (14 M) and 10 µl of Zymolyase 100T (5 mg/ml in Buffer C from Seikagaku Corp. Japan). Coverslips were prepared by incubation for 1 h in 0.1 M HCl followed by ten successive washes in water to a volume of 10× and storage in ethanol. Before cell application, all ethanol was removed and coverslips were treated with poly-L-lysine 70,000–150,000 M.W. (1 mg/ml in water; from Sigma-Aldrich) for 5 min and washed with water. Cells were then washed twice with 1 ml Buffer C, placed on the coverslips and incubated at room temperature for 7 min. Coverslips were washed once with PBS and then incubated for 10 min in blocking buffer (1× PBS, 5% fetal goat serum [Sigma-Aldrich], 1% BSA, 0.2% NP-40, and 0.002% sodium azide). Coverslips were incubated with anti-myc monoclonal antibody 9E10 (1:1,000 in 1× PBS and 1% BSA; Babco Covance) at 30°C for 90 min. They were subsequently washed four times with 1× PBS and two times with blocking buffer, and then incubated in Alexafluor anti–mouse antibody (1:1,000 in 1× PBS and 1% BSA; Molecular Probes) in the dark at room temperature for 60 min. Finally, coverslips were washed two times in blocking buffer and once in PBS, then placed on slides with Antifade (Molecular Probes). Coverslips were sealed with nail polish and viewed as above.

Electron microscopy

Yeast cells were fixed, stained, embedded and sectioned as described previously (Wright, 2000); the procedure was performed by Marc Pypaert in the Yale Cell Biology Electron Microscopy Facility. Cells were visualized on a Tecnai 12 Biotwin (FEI) at 80 kV and images were captured using a Morada CCD camera (Olympus Soft Imaging Solutions) with the help of Dr. Pypaert. Random sections were used for measuring contour distances between pores. For each nucleus, pores were identified as a break in the nuclear membrane, and the relative distances between all nearest pairs of individual pores in a section were measured from the center of one pore along the contour of the membrane to the center of the second one. Distances were normalized to total contour length, and pore–pore clustering was compared between strains using a paired *t* test.

Assay of mRNA export

Cells transformed with the appropriate *lacZ* reporter plasmid (Legrain and Rosbash, 1989; Rain and Legrain, 1997) were grown overnight in sucrose media lacking uracil, diluted to early log-phase the next morning, and transferred to raffinose media lacking uracil. Induction of *lacZ* was achieved by addition of 2% galactose for 2–3 h. The OD_{600} of each sample was measured, and aliquots were centrifuged, resuspended in 300 µl lysis buffer (0.6% Triton X-100 [vol/vol], 0.75% ONPG [wt/vol], 2.25% β-mercaptoethanol [vol/vol], and 0.15 M Tris-HCl, pH 7.5), and kept at −80°C overnight (Deng and Hochstrasser, 2006). Samples were incubated at 37°C for varying times, 150 µl 1 M Na_2CO_3 was added to stop the reaction, and debris was removed by centrifugation at 13,200 rpm. Absorbance at 405 nm was measured. Strains carrying *mlp1* and *esc1* deletions were from the *S. cerevisiae* Genome Project.

Online supplemental material

Three supplementary figures are included as online supplemental data. Fig. S1: fluorescence microscopy shows that Nsp1-GFP and Nup159-GFP partially relocalize to *esc1Δ* foci and Nup60-GFP localization is not altered by *mlp1Δ mlp2Δ*. Fig. S2: a β-galactosidase–based splicing reporter assay shows neither *esc1Δ* nor *mlp1Δ* is defective in splicing a reporter construct (pJCR51) compared with WT. Fig. S3: Western blot analysis of pULP1 (Ulp1-9myc) shows Ulp1 is expressed at similar levels in *ulp1Δ* and *esc1Δ ulp1Δ* cells. Online supplemental material is available at http://www.jcb.org/cgi/content/full/jcb.200702154/DC1.

We thank J.D. Aitchison for Nup-GFP strains; V. Panse for Ulp1C-Nup fusion plasmids; M. Pypaert for help with EM; M. Kroetz for help recording fluorescence images; A. Jacquier for the mRNA export reporters; and A. Kusmierczyk and T. Ravid for comments on the manuscript.

This work was supported by National Institutes of Health grant GM053756 to M. Hochstrasser. A. Lewis and R. Felberbaum were supported in part by National Institutes of Health training grant GM007223.

Submitted: 23 February 2007
Accepted: 25 July 2007

Table I. **Yeast strains used**

Name	Genotype (all *MATa* except where noted)	Source
AL224	*esc1Δ::kanMX ade2-1 his3-11,15 leu2-3,112 trp1-1 ura3-52*	This study
AL244	*nup2Δ::kanMX ade2-1 his3-11,15 leu2-3,112 trp1-1 ura3-52*	This study
AL379	*NUP60-GFP::his5+ esc1Δ::kanMX his3-Δ200 leu2-3,112 trp1-1 ura3-52 lys2-801*	This study
AL383	*NUP49-GFP::his5+ esc1Δ::kanMX his3-Δ200 leu2-3,112 trp1-1 ura3-52 lys2-801*	This study
AL385	*NUP159-GFP::his5+ esc1Δ::kanMX his3-Δ200 leu2-3,112 trp1-1 ura3-52 lys2-801*	This study
AL387	*NUP2-GFP::his5+ esc1Δ::kanMX his3-Δ200 leu2-3,112 trp1-1 ura3-52 lys2-801*	This study
AL389	*esc1Δ::kanMX his3-Δ200 leu2-3,112 trp1-1 ura3-52 lys2-801*	This study
AL391	*NUP49-GFP::his5+ his3-Δ200 leu2-3,112 trp1-1 ura3-52 lys2-801*	Dilworth et al., 2001
AL392	*NUP159-GFP::his5+ his3-Δ200 leu2-3,112 trp1-1 ura3-52 lys2-801*	Dilworth et al., 2001
AL397	*NUP2-GFP::his5+ his3-Δ200 leu2-3,112 trp1-1 ura3-52 lys2-801*	Dilworth et al., 2001
AL399	*NUP60-GFP::his5+ his3-Δ200 leu2-3,112 trp1-1 ura3-52 lys2-801*	Dilworth et al., 2001
AL414	*esc1Δ::kanMX yku80Δ::kanMX ulp2Δ::HIS3 ade2-1 his3-11,15 leu2-3,112 trp1-1 ura3-52*	This study
AL424	*yku80Δ::kanMX esc1Δ::kanMX ade2-1 his3-11,15 leu2-3,112 trp1-1 ura3-52*	This study
AL444	*nup60Δ::kanMX ade2-1 his3-11,15 leu2-3,112 trp1-1 ura3-52*	This study
AL454	*esc1Δ::kanMX ulp2Δ::HIS3 ade2-1 his3-11,15 leu2-3,112 trp1-1 ura3-52*	This Study
AL467	*ulp2Δ::HIS3 nup60Δ::kanMX ade2-1 his3-11,15 leu2-3,112 trp1-1 ura3-52*	This study
AL513	*NUP60-CFP::LEU2 his3-Δ200 leu2-3,112 trp1-1 ura3-52 lys2-801 esc1Δ::kanMX*	This study
AL521	*esc1Δ::kanMX ulp1Δ::HIS3 his3-Δ200 leu2-3,112 trp1-1 ura3-52 lys2-801* YCp50-ULP1	This study
AL542	*NUP49-CFP::LEU2 his3-Δ200 leu2-3,112 trp1-1 ura3-52 lys2-801 esc1Δ::kanMX*	This study
AL543	*esc1Δ::kanMX nup2Δ::kanMX ade2-1 his3-11,15 leu2-3,112 trp1-1 ura3-52*	This study
AL546	*NUP2-GFP::his5+ nup60Δ::kanMX his3-Δ200 leu2-3,112 trp1-1 ura3-52 lys2-801*	This study
AL547	*NUP49-CFP::LEU2 his3-Δ200 leu2-3,112 trp1-1 ura3-52 lys2-801*	This study
AL549	*NUP60-CFP::LEU2 his3-Δ200 leu2-3,112 trp1-1 ura3-52 lys2-801*	This study
AL561	*nup60Δ::kanMX ulp1Δ::HIS3 his3-Δ200 leu2-3,112 trp1-1 ura3-52 lys2-801* YCp50-ULP1	This study
AL564	*NUP49-GFP::His5 nup60Δ::kanMX his3-Δ200 leu2-3,112 trp1-1 ura3-52 lys2-801*	This study
AL582	*sir4Δ::kanMX ade2-1 his3-11,15 leu2-3,112 trp1-1 ura3-52*	This study
AL583	*sir4Δ::kanMX ulp2Δ::HIS3 ade2-1 his3-11,15 leu2-3,112 trp1-1 ura3-52*	This study
AL585	*NUP49-GFP::his5+ esc1Δ::kanMX nup60Δ::kanMX his3-Δ200 leu2-3,112 trp1-1 ura3-52 lys2-801*	This study
AL586	*NUP2-GFP::his5+ esc1Δ::kanMX nup60Δ::kanMX his3-Δ200 leu2-3,112 trp1-1 ura3-52 lys2-801*	This study
AL587	*NUP159-GFP::his5+ esc1Δ::kanMX nup60Δ::kanMX his3-Δ200 leu2-3,112 trp1-1 ura3-52 lys2-801*	This study
AL588	*NUP159-GFP::his5+ nup60Δ::kanMX his3-Δ200 leu2-3,112 trp1-1 ura3-52 lys2-801*	This study
MHY500	*his3-Δ200 leu2-3,112 trp1-1 ura3-52 lys2-801*	Chen et al., 1993
MHY1321	*ulp1Δ::HIS3 his3-Δ200 leu2-3,112 trp1-1 ura3-52 lys2-*801 YCp50-ULP1	Li and Hochstrasser, 1999
MHY1540	*leu2-3,112 ura3-52 lys2-801 trp1-1 his3-Δ200 ULP1-GFP::kanMX*	Li and Hochstrassser, 2003
MHY2874	*mfα1Δ::MFα1pr-LEU2 can1Δ::MFA1pr-HIS3 his3Δ1 leu2Δ0 ura3Δ0 met15Δ0 lys2Δ0 ulp2Δ::NAT*	This study
MHY2972	*his3Δ1 leu2Δ0 met15Δ0 ura3Δ0*	Tong et al., 2001
MHY4085	*MLP1-YFP ade2-1 his3-11 leu2-3, 112 trp1Δ2 can1-100 ura3-52*	Galy, et al., 2004
MHY4096	*MATα Esc1-GFP::kanMX6 Nup49::Nup49-CFP URA3* hmr Aeb 4lexA^{OP} *hmr::TRP1 trp1-1 his3-11, 15 ura3 leu2*	Taddei et al., 2004
MHY4103	*Esc1-GFP::kanMX nup60Δ::kanMX Nup49::Nup49-CFP URA3* hmr Aeb 4lexA^{OP} *hmr::TRP1 trp1-1 his3-11, 15 ura3 leu2*	This study
MHY4104	*MLP1-YFP nup60Δ::kanMX ade2-1 his3-11 leu2-3,112 trp1Δ2 can1-100 ura3-52*	This study
MHY4155	*MLP1-YFP esc1Δ::his5+ ade2-1 his3-11 leu2-3,112 trp1Δ2 can1-100 ura3-52*	This study
MHY4156a	*MLP1-YFP nup60Δ::kanMX esc1Δ::his5+ ade2-1 his3-11 leu2-3,112 trp1Δ2 can1-100 ura3-52*	This study
MHY4196	*esc1Δ::his5+ mlp1Δ::kanMX his3Δ1 leu2Δ0 met15Δ0 ura3Δ0*	This study
MHY4201	*ulp1Δ::kanMX his3Δ0 leu2Δ0 ura3Δ0 MATα* YCplac22ulp1ts	This study
MHY4225	*ulp1Δ::kanMX esc1Δ::kanMX his3Δ0 leu2Δ0 ura3Δ0* YCplac22ulp1ts	This study
YDS180	*yku80Δ::URA3 ade2-1 his3-11,15 leu2-3,112 trp1-1 ura3-52 MATα*	Unpublished data
YDS181	*yku80Δ::kanMX ulp2Δ::HIS3 ade2-1 his3-11,15 leu2-3,112 trp1-1 ura3-52*	D. Schwartz
YDS80	*ulp2Δ::HIS3 ade2-1 his3-11,15 leu2-3,112 trp1-1 ura3-52 MATα*	D. Schwartz
YDS86	*ade2-1 his3-11,15 leu2-3,112 trp1-1 ura3-52*	D. Schwartz

Table II. **Plasmids**

Plasmids	Plasmid Description	Source
pULP1-GFP	YCplac22-ULP1-GFP-kanMX	O. Kerscher
pRS426-ULP2	pRS426-ULP2, *ULP2* WT plasmid (screen)	This study
YCp50-ULP1	YCp50-ULP1, *ULP1* WT plasmid	Li and Hochstrasser, 2000
pULP1-YFP	YCplac22-ULP1-YFP	This study
pULP1	YCplac22-ULP1-9myc	Li and Hochstrasser, 2003
YCplac22ulp1ts	YCplac22-ulp1-3-33 (*NAT, TRP1*)	O. Kerscher
pULP1Δ150-403	YCplac22-ulp1Δ150-403-9myc	This study
pULP1Δ150-346	YCplac22-ulp1Δ150-346-9myc	This study
pULP1Δ346-403	YCplac22-ulp1Δ346-403-9myc	This study
pULP1-C478	YCplac22-ulp1Δ2-144-9myc	Li and Hochstrasser, 2003
pULP1-C275	YCplac22-ulp1Δ2-346-9myc	Li and Hochstrasser, 2003
pULP1-N417	YCplac22-ulp1Δ418-621-9myc	Li and Hochstrasser, 2003
pULP1-N346	YCplac22-ulp1Δ347-621-9myc	Li and Hochstrasser, 2003
pLGSD5	*2μ, URA3* (*lacZ* without intron)	Legrain and Rosbash, 1989
pJCR1	*2μ, URA3* (*lacZ* in-frame in pre-mRNA)	Legrain and Rosbash, 1989
pJCR51	*2μ, URA3* (*lacZ* in-frame in spliced mRNA)	Legrain and Rosbash, 1989
pJCR1mutBP	*2μ, URA3* (mutated branchpoint sequence)	Rain and Legrain, 1997

References

Andrulis, E.D., D.C. Zappulla, A. Ansari, S. Perrod, C.V. Laiosa, M.R. Gartenberg, and R. Sternglanz. 2002. Esc1, a nuclear periphery protein required for Sir4-based plasmid anchoring and partitioning. *Mol. Cell. Biol.* 22:8292–8301.

Bachant, J., A. Alcasabas, Y. Blat, N. Kleckner, and S.J. Elledge. 2002. The SUMO-1 isopeptidase Smt4 is linked to centromeric cohesion through SUMO-1 modification of DNA topoisomerase II. *Mol. Cell.* 9:1169–1182.

Bossis, G., and F. Melchior. 2006. Regulation of SUMOylation by reversible oxidation of SUMO conjugating enzymes. *Mol. Cell.* 21:349–357.

Bylebyl, G.R., I. Belichenko, and E.S. Johnson. 2003. The SUMO isopeptidase Ulp2 prevents accumulation of SUMO chains in yeast. *J. Biol. Chem.* 278:44113–44120.

Deng, M., and M. Hochstrasser. 2006. Spatially regulated ubiquitin ligation by an ER/nuclear membrane ligase. *Nature.* 443:827–831.

Denning, D., B. Mykytka, N.P. Allen, L. Huang, B. Al, and M. Rexach. 2001. The nucleoporin Nup60p functions as a Gsp1p-GTP-sensitive tether for Nup2p at the nuclear pore complex. *J. Cell Biol.* 154:937–950.

Dilworth, D.J., A. Suprapto, J.C. Padovan, B.T. Chait, R.W. Wozniak, M.P. Rout, and J.D. Aitchison. 2001. Nup2p dynamically associates with the distal regions of the yeast nuclear pore complex. *J. Cell Biol.* 153:1465–1478.

Dziembowski, A., A.P. Ventura, B. Rutz, F. Caspary, C. Faux, F. Halgand, O. Laprevote, and B. Seraphin. 2004. Proteomic analysis identifies a new complex required for nuclear pre-mRNA retention and splicing. *EMBO J.* 23:4847–4856.

Fahrenkrog, B., and U. Aebi. 2003. The nuclear pore complex: nucleocytoplasmic transport and beyond. *Nat. Rev. Mol. Cell Biol.* 4:757–766.

Feuerbach, F., V. Galy, E. Trelles-Sticken, M. Fromont-Racine, A. Jacquier, E. Gilson, J.C. Olivo-Marin, H. Scherthan, and U. Nehrbass. 2002. Nuclear architecture and spatial positioning help establish transcriptional states of telomeres in yeast. *Nat. Cell Biol.* 4:214–221.

Galy, V., O. Gadal, M. Fromont-Racine, A. Romano, A. Jacquier, and U. Nehrbass. 2004. Nuclear retention of unspliced mRNAs in yeast is mediated by perinuclear Mlp1. *Cell.* 116:63–73.

Green, D.M., C.P. Johnson, H. Hagan, and A.H. Corbett. 2003. The C-terminal domain of myosin-like protein 1 (Mlp1p) is a docking site for heterogeneous nuclear ribonucleoproteins that are required for mRNA export. *Proc. Natl. Acad. Sci. USA.* 100:1010–1015.

Guthrie, C., and G.R. Fink. 1991. Guide to Yeast Genetics and Molecular Biology. Academic Press, San Diego. 933 pp.

Hang, J., and M. Dasso. 2002. Association of the human SUMO-1 protease SENP2 with the nuclear pore. *J. Biol. Chem.* 277:19961–19966.

Hannich, J.T., A. Lewis, M.B. Kroetz, S.J. Li, H. Heide, A. Emili, and M. Hochstrasser. 2005. Defining the SUMO-modified proteome by multiple approaches in *Saccharomyces cerevisiae*. *J. Biol. Chem.* 280:4102–4110.

Hase, M.E., and V.C. Cordes. 2003. Direct interaction with nup153 mediates binding of Tpr to the periphery of the nuclear pore complex. *Mol. Biol. Cell.* 14:1923–1940.

Johnson, E.S. 2004. Protein modification by SUMO. *Annu. Rev. Biochem.* 73:355–382.

Kerscher, O., R. Felberbaum, and M. Hochstrasser. 2006. Modification of proteins by ubiquitin and ubiquitin-like proteins. *Annu. Rev. Cell Dev. Biol.* 22:159–180.

Krull, S., J. Thyberg, B. Bjorkroth, H.R. Rackwitz, and V.C. Cordes. 2004. Nucleoporins as components of the nuclear pore complex core structure and Tpr as the architectural element of the nuclear basket. *Mol. Biol. Cell.* 15:4261–4277.

Legrain, P., and M. Rosbash. 1989. Some cis- and trans-acting mutants for splicing target pre-mRNA to the cytoplasm. *Cell.* 57:573–583.

Li, S.-J., and M. Hochstrasser. 1999. A new protease required for cell-cycle progression in yeast. *Nature.* 398:246–251.

Li, S.-J., and M. Hochstrasser. 2000. The yeast ULP2 (SMT4) gene encodes a novel protease specific for the ubiquitin-like Smt3 protein. *Mol. Cell. Biol.* 20:2367–2377.

Li, S.-J., and M. Hochstrasser. 2003. The Ulp1 SUMO isopeptidase: distinct domains required for viability, nuclear envelope localization, and substrate specificity. *J. Cell Biol.* 160:1069–1081.

Matsuura, Y., A. Lange, M.T. Harreman, A.H. Corbett, and M. Stewart. 2003. Structural basis for Nup2p function in cargo release and karyopherin recycling in nuclear import. *EMBO J.* 22:5358–5369.

Melchior, F., M. Schergaut, and A. Pichler. 2003. SUMO: ligases, isopeptidases and nuclear pores. *Trends Biochem. Sci.* 28:612–618.

Mossessova, E., and C.D. Lima. 2000. Ulp1-SUMO crystal structure and genetic analysis reveal conserved interactions and a regulatory element essential for cell growth in yeast. *Mol. Cell.* 5:865–876.

Palancade, B., M. Zuccolo, S. Loeillet, A. Nicolas, and V. Doye. 2005. Pml39, a novel protein of the nuclear periphery required for nuclear retention of improper messenger ribonucleoparticles. *Mol. Biol. Cell.* 16:5258–5268.

Panse, V.G., B. Kuster, T. Gerstberger, and E. Hurt. 2003. Unconventional tethering of Ulp1 to the transport channel of the nuclear pore complex by karyopherins. *Nat. Cell Biol.* 5:21–27.

Pfander, B., G.L. Moldovan, M. Sacher, C. Hoege, and S. Jentsch. 2005. SUMO-modified PCNA recruits Srs2 to prevent recombination during S phase. *Nature*. 436:428–433.

Rain, J.C., and P. Legrain. 1997. In vivo commitment to splicing in yeast involves the nucleotide upstream from the branch site conserved sequence and the Mud2 protein. *EMBO J.* 16:1759–1771.

Rout, M.P., J.D. Aitchison, A. Suprapto, K. Hjertaas, Y. Zhao, and B.T. Chait. 2000. The yeast nuclear pore complex: composition, architecture, and transport mechanism. *J. Cell Biol.* 148:635–651.

Schwartz, D.C., and M. Hochstrasser. 2003. A superfamily of protein tags: ubiquitin, SUMO and related modifiers. *Trends Biochem. Sci.* 28:321–328.

Schwienhorst, I., E.S. Johnson, and R.J. Dohmen. 2000. SUMO conjugation and deconjugation. *Mol. Gen. Genet.* 263:771–786.

Smythe, C., H.E. Jenkins, and C.J. Hutchison. 2000. Incorporation of the nuclear pore basket protein nup153 into nuclear pore structures is dependent upon lamina assembly: evidence from cell-free extracts of Xenopus eggs. *EMBO J.* 19:3918–3931.

Soop, T., B. Ivarsson, B. Bjorkroth, N. Fomproix, S. Masich, V.C. Cordes, and B. Daneholt. 2005. Nup153 affects entry of messenger and ribosomal ribonucleoproteins into the nuclear basket during export. *Mol. Biol. Cell.* 16:5610–5620.

Stead, K., C. Aguilar, T. Hartman, M. Drexel, P. Meluh, and V. Guacci. 2003. Pds5p regulates the maintenance of sister chromatid cohesion and is sumoylated to promote the dissolution of cohesion. *J. Cell Biol.* 163:729–741.

Strambio-de-Castillia, C., and M.P. Rout. 2002. The structure and composition of the yeast NPC. *Results Probl. Cell Differ.* 35:1–23.

Taddei, A., F. Hediger, F.R. Neumann, C. Bauer, and S.M. Gasser. 2004. Separation of silencing from perinuclear anchoring functions in yeast Ku80, Sir4 and Esc1 proteins. *EMBO J.* 23:1301–1312.

Takahashi, H., S. Hatakeyama, H. Saitoh, and K.I. Nakayama. 2005. Noncovalent SUMO-1 binding activity of thymine DNA glycosylase (TDG) is required for its SUMO-1 modification and colocalization with the promyelocytic leukemia protein. *J. Biol. Chem.* 280:5611–5621.

Therizols, P., C. Fairhead, G.G. Cabal, A. Genovesio, J.C. Olivo-Marin, B. Dujon, and E. Fabre. 2006. Telomere tethering at the nuclear periphery is essential for efficient DNA double strand break repair in subtelomeric region. *J. Cell Biol.* 172:189–199.

Tong, A.H., M. Evangelista, A.B. Parsons, H. Xu, G.D. Bader, N. Page, M. Robinson, S. Raghibizadeh, C.W. Hogue, H. Bussey, et al. 2001. Systematic genetic analysis with ordered arrays of yeast deletion mutants. *Science.* 294:2364–2368.

Tran, E.J., and S.R. Wente. 2006. Dynamic nuclear pore complexes: life on the edge. *Cell.* 125:1041–1053.

Vinciguerra, P., and F. Stutz. 2004. mRNA export: an assembly line from genes to nuclear pores. *Curr. Opin. Cell Biol.* 16:285–292.

Wright, R. 2000. Transmission electron microscopy of yeast. *Microsc. Res. Tech.* 51:496–510.

Zhang, H., H. Saitoh, and M.J. Matunis. 2002. Enzymes of the SUMO modification pathway localize to filaments of the nuclear pore complex. *Mol. Cell. Biol.* 22:6498–6508.

Zhao, X., C.Y. Wu, and G. Blobel. 2004. Mlp-dependent anchorage and stabilization of a desumoylating enzyme is required to prevent clonal lethality. *J. Cell Biol.* 167:605–611.